Innovative processes for electropolishing of medical devices made of stainless steels

Noam Eliaz, Oded Nissan
Biomaterials and Corrosion Laboratory, School of Mechanical Engineering, Tel-Aviv University, Ramat Aviv, Tel-Aviv 69978, Israel

Received 28 December 2006; revised 26 March 2007; accepted 2 April 2007
Published online 13 June 2007 in Wiley InterScience (www.interscience.wiley.com). DOI: 10.1002/jbm.a.31429

Abstract: Currently, many medical devices are made of implantable metals such as 316LVM stainless steel. Electropolishing is a common process to obtain a smooth surface, free of contaminants and more passive, which allows for minimizing the foreign body response and cell adhesion. However, polishing of small implants with a highly complicated geometry and nonuniform metallurgy might result in unsatisfactory results. The objective of this work was to develop an electropolishing process effective for complex metallic implants such as artificial heart valve frames and miniature glaucoma implants. Polishing in an ultrasonic bath and pulsed voltage polishing processes were studied and compared to the standard ASTM process. Current-voltage curves were constructed for different solutions and bath temperatures. The polished parts were evaluated by stereomicroscopy, optical microscopy, atomic force microscopy, noncontact surface profilometry, and X-ray diffraction. Pulse polishing was found useful in eliminating the erosion effects of gas bubbles in solution. Electropolishing in an ultrasonic bath was found useful when a rough, patterned surface is needed, e.g. for osseointegration purposes. Preliminary animal studies followed by histopathology indicated that the polished surfaces stimulated only a moderate body reaction, as desired in such applications. The pronounced dependence of the measured roughness values on both the measurement technique and scanned area should inspire the preparation of a new test-method standard. © 2007 Wiley Periodicals, Inc. J Biomed Mater Res 83A: 546–557, 2007

Key words: electropolishing; stainless steel; atomic force microscope; surface roughness; cell adhesion

INTRODUCTION

Electropolishing (EP), also known as electrochemical polishing or electrolytic polishing, is the process of smoothing a metal surface anodically, while the workpiece is immersed in an appropriate solution.[1–3] The advantages of this process include: (1) Removal of material from the surface without introducing plastic deformation and residual stresses. In fact, surface modification that has been introduced during preceding mechanical grinding and polishing processes (e.g. nonuniformly deformed layer, residual stresses and surface tension) can be eliminated. Moreover, phase transformations and heating damage, which might result from severe mechanical grinding and polishing, are avoided. (2) Removal of edge burrs and unstable oxides. (3) Soft metals, which are otherwise difficult to grind and polish, can be processed. (4) Articles with small dimensions and complex geometries can be polished. (5) Improvement of the appearance and reflectivity. In stainless steels, for example, mirror-like finish can be obtained. (6) Improvement of passivation and corrosion resistance. Several ASTM standards report on passivation of stainless steels and cobalt-based alloys by EP, and even omit the nitric acid rinse (i.e. chemical passivation) requirement if EP is conducted as the final processing stage.[4–6] In stainless steels, for example, preferential etching of iron and nickel results in chromium enrichment at the surface, and formation of better, continuous, passive layer. (7) Because the surface roughness is decreased, the resistance against bacteria growth is increased. In addition, contaminants are removed from the surface, and the article may demonstrate improved sterilization.[7] (8) Allows for improved quality control by exposing defects in welds and base material.[7] (9) Once the process is optimized, automated, reproducible production can be attained. Electropolishing also has several drawbacks, including: (1) Difficulties in polishing multi-phase materials because of different material removal rates. (2) Some features, including edges and micro-cracks, might change shape and/or

Correspondence to: N. Eliaz; e-mail: neliaz@eng.tau.ac.il

expand. (3) Many solutions currently in use are toxic, or require special treatment procedures.

The success of any EP procedure depends on several parameters[8]: (1) The initial surface finish and article's geometry. Typically, rougher and sharper areas are removed preferentially. (2) The chemical composition of the solution. There are different solutions for different metals, which involve different applied voltages and processing time, throwing powers, viscosities, handling precautions, costs, etc. (3) Solution age. (4) Bath temperature. The viscosity of the solution decreases as the temperature is increased, thus allowing faster diffusion of ions and molecules in the solution, according to the Stokes-Einstein law,[9] and consequently - a higher polishing speed. In addition, heating typically leads to accelerated electrochemical reactions and enhanced gas bubble generation. The flow of bubbles at or in vicinity to the surface of an article leads to local agitation and increased current density. (5) The anode-to-cathode surface area ratio, the geometry of both electrodes, and their relative position in the bath. The cathode surface area is typically four times larger than the anode surface area, at least. Smaller areas ratio involve lower current densities and might lead to electrochemical etching, instead of EP. (6) Current density. A higher applied current density will result in a higher material removal rate, until a limiting current density is reached. (7) Polishing time, which typically affects almost linearly the extent of material removal. (8) Agitation of the solution.

The mechanisms of EP are discussed with the aid of Figure 1, which illustrates the "polishing layer" and its thickness dependence on the initial surface roughness of the workpiece. When a metal is immersed in an aqueous solution, some metal atoms are oxidized, releasing cations to the solution. Because of the accumulation of electrons, the metal surface acquires a negative electric potential, which - in turn - attracts the cations and terminates the dissolution process. Thus, a thin capacitive layer ("double layer") forms at the metal/solution interface. If the metal is connected to a power supply, which consumes the excess electrons from it, the anodic dissolution can proceed. In such "electrolytic cell," the anode is the positive terminal and the cathode is the negative terminal.[10] Because the metal is maintained at a potential that is positive relative to its equilibrium potential, there is a net flux of cations from the metal into the solution. The viscosity of the solution is responsible for a thin layer, immediately adjacent to the surface of the workpiece, that does not partake in the general agitation of the solution. Consequently, the dissolved ions must travel through this layer by diffusion before they can reach the bulk solution. The thickness of this layer, known as the Nernst diffusion layer, is a function of the

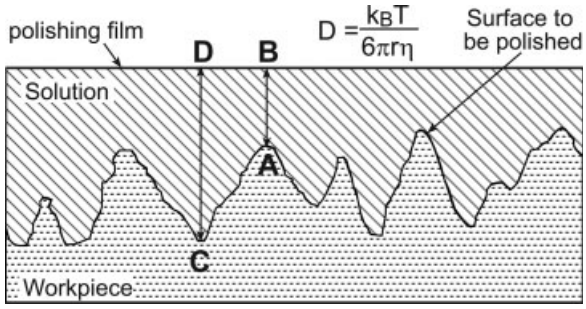

Figure 1. Schematic description of the polishing layer and its thickness dependence on the initial surface roughness of the workpiece. Note: the top boundary line is not straight in practice.

kinematic viscosity and agitation of the solution, as well as of the limiting current density. In a conventional electrochemical cell with moderate stirring the thickness is in the range of 50–100 μm. However, small inter-electrode gaps and high linear flow velocities of the solution can significantly reduce this thickness. The Nernst diffusion layer (also referred herein as the "polishing layer") is enriched with anodic dissolution products, and has higher viscosity and greater electrical resistivity compared to the bulk solution. As the metal potential is increased, the thickness of the polishing layer is also increased. Eventually, a stage is reached where, for any further increase of potential, the current of released cations does not increase anymore. At this stage, the thickness of the polishing layer controls the dissolution rate, and the dissolution becomes selective.

It is common to describe a surface, where the height of the asperities is of the order of the thickness of the Nernst diffusion layer, as macro-rough; such asperities are therefore defined as macro-asperities. Similarly, a surface, where the height of the asperities is significantly less than the thickness of the Nernst diffusion layer, is described as micro-rough; such asperities are defined as micro-asperities. Jacquet[11] suggested that at macro- and micro-asperities, the dissolution rate is higher because the thickness of the insulating polishing layer is smaller, and the electric field is higher (Fig. 1). Elmore[12,13] suggested another mechanism for EP, according to which surface leveling is controlled by the diffusion distances of anodic dissolution products from the anode through the polishing layer. Baumann and Ginsberg[14] criticized Jacquet's theory and suggested that surface leveling occurs due to greater dissolution probability at peaks. Edwards[15] criticized Elmore's theory and postulated that EP processes are governed by the diffusion of acceptors such as $(H_2PO_4)^-$, $(HPO_4)^{2-}$, and $(PO_4)^{3-}$ to the anode surface. The polishing rate is thus determined by the mobility of the acceptor toward the anode.

Because the acceptor concentration gradient is higher on peaks than on valleys, leveling occurs. Wagner[16] suggested the first mathematical description of EP, in which the surface roughness is described by a sine-wave profile. The theory predicts a linear plot for the metal loss per unit area *versus* the ratio between the amplitude at time $t = 0$ and the amplitude at time t, the amplitudes ratio being presented in a logarithmic form. In modern electrochemistry, EP is explained on the basis of new concepts of anodic passivity of metals. Because of the chemical dissolution of the passivating oxide layer in the solution, the metal does not assume a steady stable passivation state during EP. Thus, surface leveling takes place because the passivation of wells is more stable and inhibits etching.

Jacquet[17] suggested that EP should better be conducted under constant voltage conditions, rather than under constant current density conditions. However, it should be realized that this requires a careful control of the process parameters due to the possible effects of the resistance and activation overpotentials.[10] It is nowadays a common practice to apply the highest potential possible within the passivity regime of the potential *versus* log (current density) curve, or anode current density *versus* cell voltage curve, for a metal with an active-to-passive transition. At this potential, the current is nearly constant, and the oxygen evolution reaction is insignificant (it becomes a concern at a more positive potential, within the transpassive regime).

The biomaterials market for cardiovascular devices was estimated in the year 2002 at 6 million dollars in the U.S. alone. Approximately 100,000 heart valves and 1.5 million coronary stents were implanted in the U.S. during that year.[18] Stainless steels, such as 316LVM (where L designates low carbon content, and VM stands for vacuum melted),[19,20] have been widely used in such applications. In recent years, new minimally invasive and transapical aortic heart valve replacement technologies have been emerged.[21] In such cardiovascular applications, protein adsorption and the subsequent cell adhesion should be inhibited to minimize the risk of neointimal hyperplasia and stenosis. A smooth surface can aid in preventing the activation and aggregation of platelets, which is recognized to be a stage in thrombosis.[22,23] One way to achieve this goal is by EP of the device. On the other hand, cell adhesion and cell proliferation can be improved by increase of the surface roughness on a nanometer scale.[24] This is important, in particular, in applications where a strong tissue-device bond is required (for example, for osseointegration of orthopedic and dental implants). Hence, there is interest also in processes for roughening and texturing of surfaces (such as grit blast).

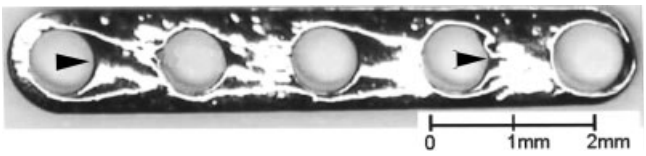

Figure 2. Hanging wire mark and oval shapes because of gas bubble flow along a heart valve frame bar made of 316LVM and electropolished via a standard DC process.

Electropolishing of modern miniature surgical implants may be challenging because of the small dimensions, complex geometries, and the use of processes, such as laser cutting, that introduce metallurgical nonuniformities. Figure 2 demonstrates two of the possible shortcomings in conventional EP. This figure shows a part (5-hole bar) from the frame of a percutaneous heart valve made of 316LVM. The manufacturing of this part includes laser-cutting from seamless tube, holes rounding by stamping, and EP. The sample shown in Figure 2 was electropolished in a commercial solution ("BO" solution from Limat Metal Surface Treatments) at 70°C, with no stirring, following a conventional direct current (DC) EP procedure. The samples were hung on nitinol wires. Problems that were observed include: (1) poor reproducibility, (2) incomplete polishing, (3) distortion of the holes through which the sample holder (wire) was connected, (4) marks from the sample holder (Fig. 2), and (5) oval shapes because of the evolution of gas bubbles along the surface (Fig. 2). Commercial confidentiality considerations have limited significantly the publications on EP of medical devices. In addition to seeking for relative advantage in the large market of biomaterials and medical devices, it is difficult to protect innovative EP technologies by patents.

In the absence of proven solutions to the EP problems that had been encountered, it was decided to develop new EP procedures in-house. The primary goal was to form heart valve frames with surface finishes better than those that are obtainable by conventional DC-EP procedures, in a simple, reproducible manner. However, secondary targets were also defined, as follows: (1) To design special grippers for polishing the bars of the heart valve frames to allow batch, reproducible EP, while eliminating the effects of contact points between the hanging wires (former grippers) and the samples. (2) To suggest a set-up for EP of the frames with an integrated system controlled through a virtual instrument (such as National Instruments' LabVIEW graphic interface) on a PC. (3) To achieve a final surface finish of N2 ($R_a = 50$ nm) or better for the bar, and N1 ($R_a = 25$ nm) or better for the rest of the frame. (4) Sample thinning of no more than 30 μm. This article focuses on target No. 3 only.

Two approaches were studied and compared to the conventional ASTM process. The first approach was to immerse the EP cell in an ultrasonic (US) cleaning tank. By using an electrical generator that produces a high-frequency signal (typically, 20–250 kHz), a piezo ceramic transducer rapidly induces compression and rarefaction waves in the fluid. Millions of microscopic cavitation bubbles are formed in the fluid and release enormous energy upon collapse. Because the waves propagate in the fluid nearly without any preferred direction, it was assumed that gas bubbles (e.g. related to the oxygen evolution reaction) will be removed from the surface of the workpiece efficiently and uniformly, thus eliminating the phenomenon of oval-shape polishing. A reference was tracked for EP aided by US energy, which had been found effective in preventing reaction byproducts from attaching to the electrode, in shortening the polishing cycle time for each workpiece, and in improving the surface roughness of the workpiece.[25] However, the results claimed in the patent are much different from those found in the present work, as demonstrated below.

The second approach reported herein is pulse EP. Pulsed (or periodic reverse pulsed) current/voltage profiles have been applied extensively in electroplating during recent years.[10] In addition, Burstein et al.[26] have used pulsed voltages to anneal 304L stainless steel electrochemically. Yet, the authors are not familiar with any journal publication in which pulse EP was evaluated in general, or with respect to forming of medical devices specifically. Pulse EP may allow release of heat and reaction byproducts at each off-current interval, thus employing a lower average electric current density compared to conventional EP. During the off-current interval, the growth of reaction gas bubbles and their accumulation at the surface of the workpiece can be limited, thus improving the surface finish. Other potential advantages include the extension of the operating range of a given solution, and the achievement of a more uniform polishing of articles with complex geometries. However, extended polishing time (due to off-current intervals) and relatively small metal removal rates might limit the use of pulse EP in some cases. A two-step electromachining and electropolishing process, in which macro-asperities were first removed using short pulses, and micro-asperities were subsequently removed by either longer pulses or a DC, has been patented.[27] Reverse pulse EP has also been patented for electromachining.[28]

EXPERIMENTAL

A model 2425 digital SourceMeter® from Keithley Instruments was used to source the current/voltage. This 100 W instrument allows application of up to 1.05 A in the 105 V range, or up to 3.15 A in the 21 V range. A Lauda Ecoline E-220T thermostatic bath was used to stabilize the solution temperature at $\pm 0.1^{\circ}C$. A pure platinum wire (0.3 mm in diameter) was used to hold the specimens. The cathode was 2×2 cm^2 foil of pure platinum, which was welded to a platinum wire for contact. The surface area of the cathode was much larger than the surface area of the anode (the bar to be polished), namely 8 cm^2 *versus* 0.27 cm^2, respectively. A commercial "BO" solution was selected for the major part of work because it is fairly safe to handle (namely, it contains neither hydrofluoric acid nor perchloric acid). As a control group, some samples were electropolished in a 50:50 (vol %) sulfuric acid (96%): orthophosphoric acid (85%), in accordance with ASTM B 912.[5] Experiments were also carried out in 200-mL DI water:590-mL glycerol:100-mL orthophosphoric acid (85%), as well as in commercial PolyGard solution. The solution was replenished before each working day and once its level in the cell decreased below a predetermined level during the experiment, to avoid enrichment with reaction products. An ultrasonic cleaner model UR 1 from Retsch GmbH (operation frequency 35 kHz, volume 5.7 L) was used in part of the work. The density of cavitation bubbles-induced energy was adjusted roughly by control of the volume of water in the cleaner.

The EP cell was contained in a 250 mL glass beaker. Whereas the standard EP was carried out at $75^{\circ}C$,[5] the effect of bath temperature on the nonstandard processes was evaluated at 40, 50, 58, and $67^{\circ}C$. At each temperature, current *versus* voltage curves were constructed for four samples, to ensure reproducibility. After comparison of curves, however, only one temperature that allowed for higher current densities and good polishing was applied consistently. In the standard procedure, either the applied current density was maintained at 0.15 A cm^{-2} (which is the slowest recommended one),[5] or the applied voltage was kept constant within the range 2–4 V for less than a minute and up to 10 min. For the nonstandard procedures, however, preliminary current *versus* voltage curves were constructed within the range 0–9 V at voltage scan rates of 0.5–40 mV s^{-1}. While the slowest scan rates allowed for identification of fine features in the curves, they resulted in longer experiments and enhanced removal of metal. Therefore, the results reported herein for the nonstandard procedures relate to a scan rate of 40 mV s^{-1}. To achieve target No. 4 for the maximum metal removal allowed, preliminary thickness and weight measurements (by Sartorius model Basic BA 210 S balance with a precision of 0.1 mg) were carried out before and after EP. From these measurements, the necessary polishing time was estimated. Typical EP times were 5 min and less than 1 min for pulse and DC polishing, respectively. Following EP, the samples were rinsed twice in hot water and dried.

Following EP, several characterization techniques were used. All polished samples were imaged by means of stereo-microscope, digital camera and optical microscope (Olympus model IX 71) - under either Bright Field or Differential Interference Contrast. Atomic force microscope (AFM, model PicoSPM™ from Molecular Imaging, contact mode, scanned area 4.8×4.8 $(\mu m)^2$), in combination with SPIP ver. 3.0.0.11 software from Image Metrology A/S, were used to construct Abbott-Firestone Curves[29] and mea-

sure the amplitude parameters of mean roughness (R_a) and root-mean-square roughness (Z_{rms}). The two amplitude parameters represent an overall measure of the texture comprising the surface, and are defined mathematically as:

$$R_a = \left(\frac{1}{N}\right)\sum_{i=1}^{N}|Z_i - \overline{Z}| \quad (1)$$

$$Z_{rms} = \left[\left(\frac{1}{N}\right)\sum_{i=1}^{N}(Z_i - \overline{Z})^2\right]^{1/2}, \quad (2)$$

where $\overline{Z} = \left(\frac{1}{N}\sum_{i=1}^{N} Z_i\right)$, Z_i is the height at coordinate (x,y), i is the serial number of measurement, and N is the number of data points in the scanned area (or in the whole profile, in the case of R_a). Whereas R_a is typically used to characterize machined surfaces, Z_{rms} is typically used to specify optical surfaces. It should be noted that scanning tunneling microscopy (STM) has already been standardized to determine the surface roughness of components made of stainless steel on the nanometer scale.[30] The Abbott-Firestone Curve, also known as the Bearing Area Curve (or Bearing Ratio Curve), is the integral of the amplitude distribution function (i.e. it is a cumulative probability distribution). Ordinarily, the integral is performed from the highest peak to the lowest valley, so each point on the curve has the physical significance of showing what linear fraction of a profile lies above a certain height. Surface texture parameters that can be deduced from the curve include: the core roughness depth (S_k), which is a measure of the nominal, or "core", roughness (peak-to-valley) of the surface with the predominant peaks and valleys removed; the reduced peak height (S_{pk}), which is a measure of the peak height above the core roughness; the reduced valley depth (S_{vk}), which is a measure of the valley depth below the core roughness; and the height difference between two points with different percent bearing ratio, along the abscissa (e.g. $S_{dc}0\_5$, $S_{dc}5\_10$, $S_{dc}10\_50$, $S_{dc}50\_95$).[31]

The surface finish was characterized also by means of a noncontact profiler model NewView 200 with MetroPro software from Zygo Corp. This profiler is based on scanning white-light interferometry and provides a three-dimensional (3D) image of the surface. The scanned area ranged from 40×50 μm^2 to 190×260 μm^2, and the camera resolution from 0.2 to 0.811 μm. On each side of the bar, several measurements were conducted along the center long axis and in vicinity to the holes' circumference. To compare between different samples with respect to possible existence of residual micro-strains and residual microstresses, X-ray diffraction (XRD) was carried out on selected samples. To this aim, a Θ-Θ powder diffractometer from Scintag, equipped with a liquid nitrogen-cooled germanium solid-state detector and Cu-K_α radiation source ($\lambda = 1.5406$ Å), was used. The data was collected at a scan rate of 1 deg min^{-1}, from $2\Theta = 20$ to 100°. Identification of reflections was made by comparison to JCPDS (Joint Committee on Powder Diffraction Standards) cards 06-0696 (ferrite), 23-0298 and 31-0619 (austenite), 44-1291, 44-1292, and 44-1293 (martensite). A peak shift to lower diffraction angles may be associated with tensile residual strains. By recording the peak shift as a function of sample tilt angle, the residual stress can be determined using isotropic elasticity theory. In this work, however, only a simple comparison of the full width at high maximum (FWHM) and position of peaks was employed, focusing on high reflection angles - to increase the accuracy.

In an attempt to predict the body reaction to the electropolished bars, selected bars were implanted in rattus species. It should be emphasized that only a few preliminary *in vivo* studies were carried out, therefore the results cannot be referred to as statistically significant. Four types of bars were analyzed: unpolished, US-EP in "BO" solution, pulse EP in "BO" solution, and pulse EP in PolyGard solution. Prior to surgery, the bars were cleaned ultrasonically in ethanol (70%), dried, sterilized in ethylene oxide (EtO) gas, and packed in a clean room. These procedures were carried out at BrainsGate (Ra'anana, Israel). Each bar was then implanted subcutaneously in the hip region of a separate adult rattus (weight ~550 g, performed at Pharma Seed, Nes Ziona, Israel). After dissection of the skin-muscle flap, the bar was inserted and knotted by means of a nylon wire, and the wound was closed by sutures. Following a 14-days implantation, the bars with their surrounding tissues were removed and sent for histopathology analysis (Patho Vet Diagnostic Veterinary Pathology Services, Kfar Bilu, Israel). The implanted material was removed from all sections after fixation and before histological processing. The remaining tissue was sectioned transversally in two areas (where the space from implant was grossly evident).

RESULTS AND DISCUSSION

First, the current *versus* voltage curves are evaluated to select the proper voltage for EP. Figure 3 compares typical curves that were obtained for the 316LVM stainless steel bars in "BO" solution at four different temperatures. It is evident that as the temperature is raised from 40 to 50°C, a polishing range becomes well defined at a lower voltage. When further increasing the temperature to 58°C, the current density is increased at a fixed voltage. A further increase of temperature to 67°C did not lead to a significant change in current density. The change in current density as a function of temperature can be explained in terms of the viscosity of the solution, which decreases at elevated temperatures. Usually, the lowest temperature that yields good polishing in a reasonable time frame is selected before, to be as far as possible from boiling conditions and allow for a convenient, safe work. Therefore, the subsequent EP work was conducted at a fixed temperature of 58°C. It should be noted that at high voltage scan rates, the peak in the current *versus* voltage curve disappeared, and the curve only contained an inflection point that distinguished between a behavior of a soluble anode at low voltages and a behavior of an insoluble anode at high voltages. Moreover,

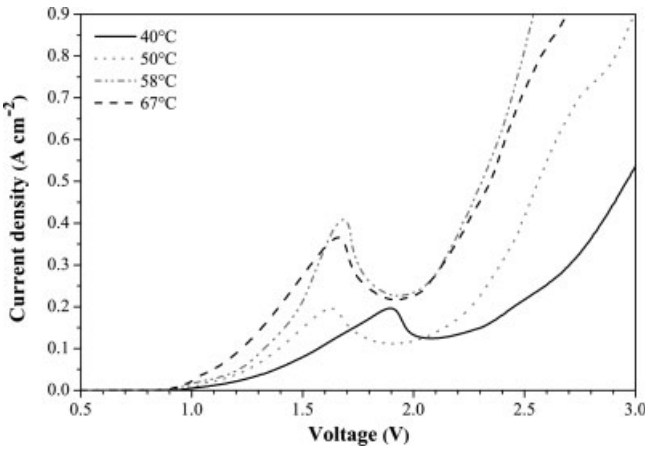

Figure 3. The typical temperature dependence of the current *versus* voltage curves for 316LVM bars in commercial "BO" solution.

high-resolution inspection of Figure 3 revealed two inflection points within the range 1.5–1.8 V. Such a complex behavior, which might have been overlooked in the literature, can be related to contributions from different phases that exist on the surface (e.g. the austenitic phase and an amorphous phase, the latter being a result of laser cutting). Finally, with respect to the current *versus* voltage curves, it should be noted that curves constructed while the EP cell was immersed in an operating ultrasonic cleaning tank were noisy.

Figure 4 shows macroscopic images of four representative samples. Figure 4(a) shows an as-received, unpolished bar. A rough surface and randomly oriented scratches are evident. Figure 4(b) shows a bar that was polished by the standard DC process. The surface is visually smoother than the surface of the unpolished sample. Note the effects of the specimen holder (wire) in the second and fourth holes, and of the flow of gas bubbles along the bar, both being similar to the effects already noticed in Figure 2. Altogether, most samples polished by means of the standard DC-EP process were found to be either nonuniform or not smooth enough. Figure 4(c) shows a bar that was polished by the nonstandard US-EP process. Neither scratches nor specimen holder or bubble flow effects can be seen. This sample looks more uniform, but rougher, than the unpolished sample. Inspection of the long-transverse section showed that the thickness was reduced uniformly along the sample. The US process was also found to remove material evenly along the circumference of holes, thus maintaining their shape and sharp edges. It should be noted that the US process was found to be less sensitive to small variations of voltage compared to the standard EP process. The amount of metal removed by the US process was found to decrease either as the bath temperature was decreased, or as the density of energy produced by cavitation bubbles was decreased. The effects reported herein are markedly different from those reported in a former patent.[25] The microscopic texturing (cratering) observed in the present study can be attributed to:

1. Nonuniform activity of the polishing layer along the surface of the sample because of the presence of standing (stationary) waves, which do not involve net propagation of energy, in solution. Standing waves can arise if the medium is moving in an opposite direction to the wave, or as a result of interference between two waves traveling in opposite directions in a stationary medium.
2. Micro-cavitation because of the combined effect of compression waves in the US bath and tiny bubbles that are generated during the electrochemical process. In this case, one can expect the US-EP process to introduce residual compression stresses to a thin layer just beneath the surface, thus improving the durability of the article under fatigue conditions. The combination of a uniformly cratered surface and improved fatigue resistance can be taken advantage of, for example, in load-carrying metal implants that should provide a strong bond with bone via either direct morphological fixation or enhanced adhesion to a top bioactive coating.

The second nonstandard approach reported herein is pulse EP. As a starting point for process development, conditions that resulted in the best polished

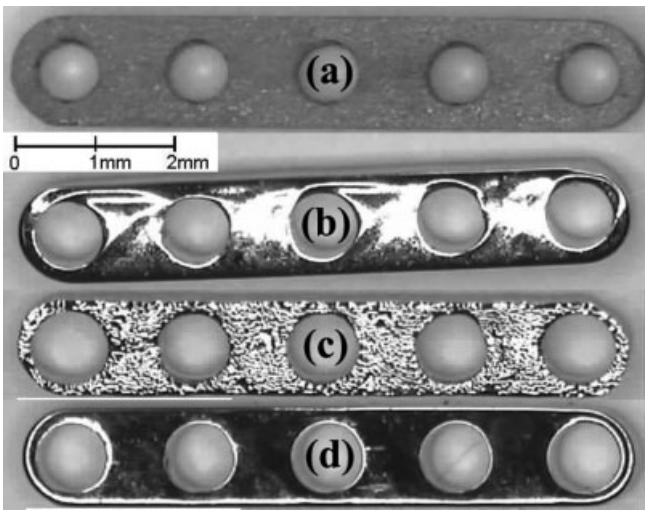

Figure 4. Macroscopic view of the bar samples: (a) before EP, (b) after standard DC-EP process, (c) after nonstandard EP process in an ultrasonic bath, (d) after nonstandard, pulsed voltage, EP process.

samples by the standard process were tuned. Pulse EP was found to allow working at higher voltages compared to the standard EP process, while still achieving good polishing. The effect of gas bubble flow along the surface was eliminated in pulse EP. In contrast to the US process, sharp edges were rounded during pulse EP. Figure 4(d) shows a bar that was polished by the nonstandard pulse EP process. The polishing conditions in this case were: 5 V applied voltage, 1 s on-current interval, 5 s off-current interval, 120 cycles (the sample being turned over after 60 cycles to achieve more symmetrical polishing effects). The bar polished this way was visually uniform, smooth, and demonstrated no signs of gas bubble flow or through-hole gripping.

Figure 5 shows typical 3D images of the surfaces of the bars shown in Figure 4, as acquired by surface profilometry. It should be emphasized that white-light interferometry measurements are affected by the metal reflectivity, and might therefore introduce artifacts. It is evident that the standard DC-EP [Fig. 5(b)] made the surface smoother, when comparing to the unpolished bar [Fig. 5(a)]. The bar polished by the US-EP process [Fig. 5(c)] exhibits the roughest surface, with well defined craters. The bar polished by pulse EP [Fig. 5(d)] seems to be slightly rougher, but less wavy, than the bar polished by standard DC-EP. However, the larger scanned area in Figure 5(d) may be the cause of, or at least contribute to, this difference. The values (average ± standard deviation) of the mean roughness and root-mean-square roughness are summarized in Table I, comparing the data from surface profilometry to data from AFM. Although R_a is more relevant than Z_{rms} in the design of the artificial heart valve frame, the values of the latter are also provided in Table I, for general impression. For comparison, de Scheerder et al. used profilometer and measured $R_a = 140 \pm 20$ nm and $R_a = 40 \pm 10$ nm for stents made of 316LVM in the as-received and electropolished conditions, respectively.[22] Rohly et al. used AFM and measured $R_a =$ 217 nm and $R_a = 111$ nm on 316L stainless steel for biomedical applications in the as-received and enhanced passivation conditions, respectively.[32]

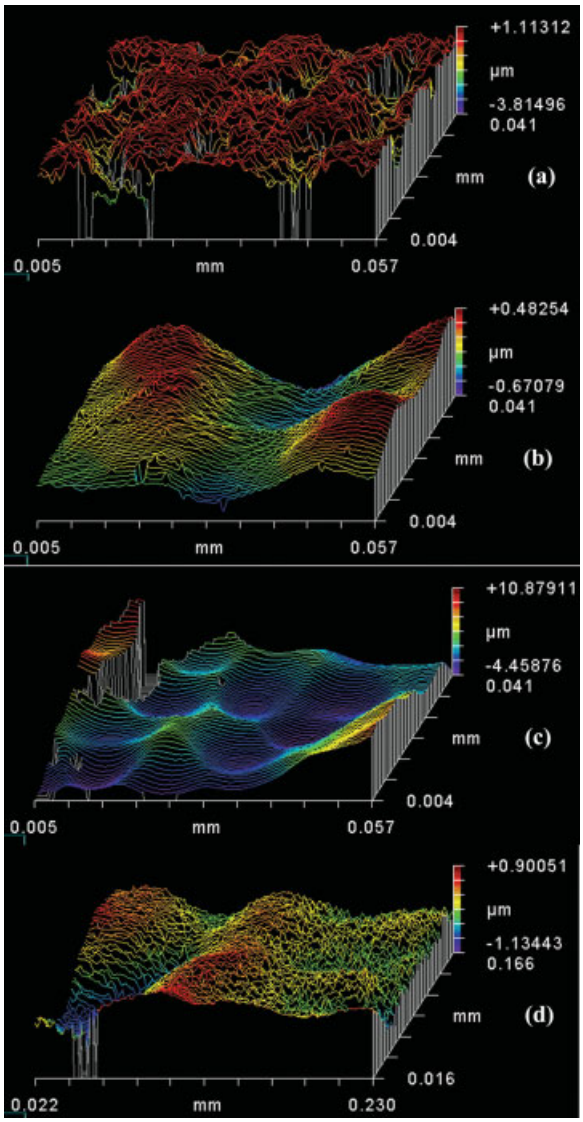

Figure 5. Typical 3D images from surface profilometer: (a) before EP, (b) after standard DC-EP process, (c) after nonstandard EP process in an ultrasonic bath, (d) after nonstandard, pulsed voltage, EP process. [Color figure can be viewed in the online issue, which is available at www.interscience.wiley.com.]

Figure 6 shows typical Abbott-Firestone curves for the same four bars, based on AFM tests. The corresponding topography and deflection images that were acquired first are not presented herein. From Figure 6(a) it is evident that the curve of the unpolished bar has a relatively steep slope, the peaks being as high as ~280 nm (120 nm at 50%). The standard DC-EP [Fig. 6(b)] resulted in a distribution of lower values (maximum ~20 nm, 8 nm at 50%). The nonstandard US-EP [Fig. 6(c)] resulted in a distribution of higher values (maximum 280 nm, 140 nm at 50%). The nonstandard pulse EP [Fig. 6(d)] resulted in a relatively flat curve (maximum 28 nm, 13 nm at 50%), which indicates a fairly uniform surface texture. Although the roughness of the pulse electropolished bar is slightly higher than that of the bar polished by conventional DC-EP, further optimization of the pulse profile may result in at least as good roughness values, while taking advantage of the removal of bubble marks. The values of the mean roughness and root-mean-square roughness, that were calculated based on AFM topography images, are summarized in Table I. From these values it is evident that both the conventional DC-EP and the nonstandard pulse EP result in surfaces that are significantly smoother than the unpolished

TABLE I
Comparison Between Roughness Measurements Made by AFM and by Noncontact Surface Profilometry

	AFM		Profiler	
Sample Type	R_a (nm)	Z_{rms} (nm)	R_a (nm)	Z_{rms} (nm)
As-received, before electropolishing	18.4 ± 4.5	23.5 ± 5.1	183.1 ± 80.6	220.1 ± 93.6
After standard DC-EP	2.1 ± 0.8	2.4 ± 0.4	76.2 ± 67.9	89.8 ± 80.2
After nonstandard US-EP	31.3 ± 2.7	34.7 ± 2.8	668.9 ± 143.8	897.0 ± 206.3
After nonstandard pulse EP	3.9 ± 3.0	3.7 ± 3.0	129.4 ± 14.7	151.0 ± 19.8

surface (DC-EP resulting in the finest surface). The nonstandard US-EP process, on the other hand, results in the most textured surface. These trends match the results from surface profilometry. The values of the amplitude parameters shown in Table I are smaller than those deduced from the Abbott-Firestone curves (note, in particular, the height at a bearing ratio of 50%, which is sometimes used for quality control). It is important to note that if quality assurance would be performed based on the amplitude parameters from this AFM data alone, all four specimens (including the unpolished and ultrasonically polished samples) would meet the design requirement of surface finish N2. On the other hand, if quality assurance would be performed based on the profiler's data, none would meet the design requirement! If the height at a bearing ratio 50% would be used as the measure, then only the DC-EP and pulse-EP samples would meet the design criterion of N2 or finer (in fact, they would both be classified as N1, whereas the unpolished and US-polished bars would be classified as N4).

As shown, the difference between roughness values obtained from AFM and those obtained from light profilometry for different scan areas is prominent. In general, larger scan areas (profiler) are expected to yield higher roughness values than smaller scan areas (AFM). ASTM F 1438,[30] for exam-

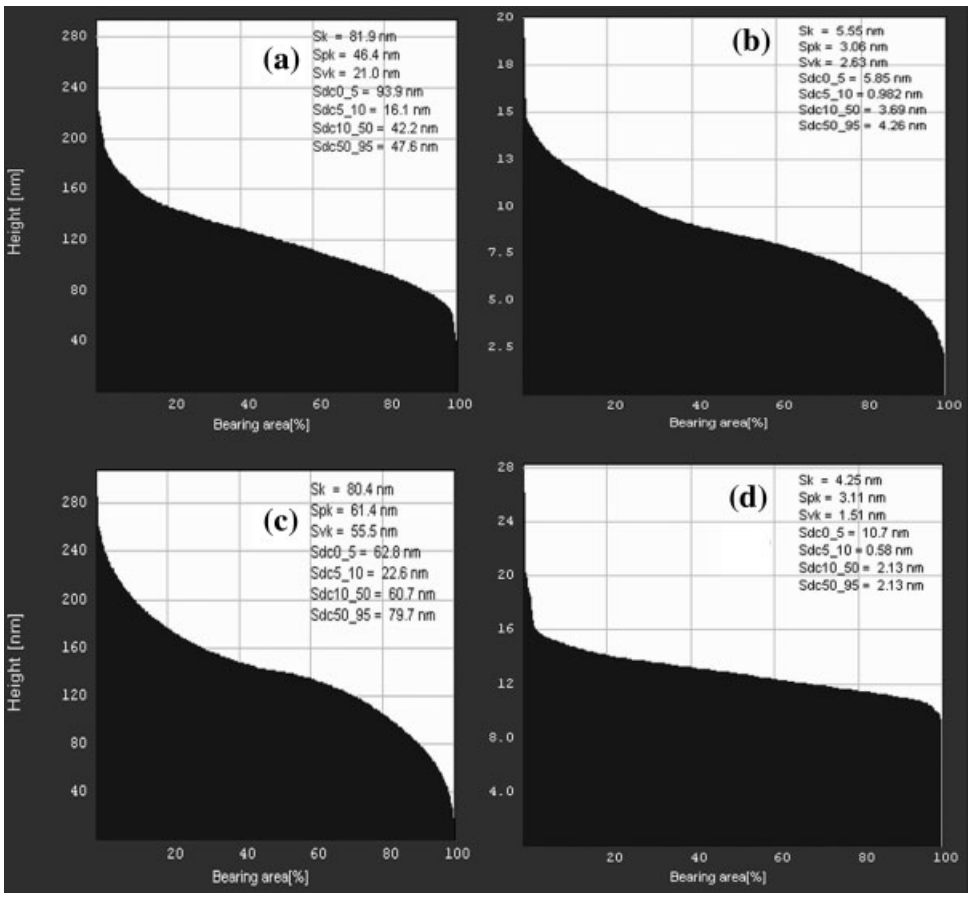

Figure 6. Typical Abbott-Firestone curves constructed following AFM imaging of bars: (a) before EP, (b) after standard DC-EP process, (c) after nonstandard EP process in an ultrasonic bath, (d) after nonstandard, pulsed voltage, EP process.

ple, reports an increase in the measured roughness of electropolished 316L stainless steel when the scanned area is increased, and therefore suggests scaling of the results relatively to the scanned area. The values of R_a and Z_{rms} reported in the standard increased from 0.71 and 1.0 nm to 0.74 and 1.9 nm, respectively, when the scanned area was increased from 0.5×0.5 μm^2 to 2.0×2.0 μm^2. A further increase in the scanned area to 20×20 μm^2 resulted in an increase in Z_{rms} to 40–630 nm. Furthermore, Kühle et al.[33] discuss several differences between AFM and interference microscopy that might result in different roughness values, even for the same area (for example, on a polished hip joint prosthesis). For AFM, deviations from real values might be due to the finite size of the probing tip, the specimen surface being not infinitely hard, or the interaction between the specimen and the tip being influenced by charging, friction and capillary forces. In the case of interference microscopy, on the other hand, the image is not a response to the surface, but depends on the reflectivity of the specimen material and the wavelength of light. Without a Gaussian filtering of the AFM image, the appearance and calculated roughness were significantly different from those of interference microscopy (the average roughness from AFM being 77% higher). However, by using an effective cut-off wavelength to filter the AFM image, the calculated roughness values became equal. Bourauel et al.[34] made a comparison between the Z_{rms} of orthodontic archwires made of Ni-Ti, stainless steel and β-titanium alloy, as measured by AFM, laser specular reflectance and stylus surface profilometer. The scanning distance in profilometry was 5.0 mm, while the area scanned by AFM was 100×100 μm^2. The smoothest (stainless steel) wire was found to have a roughness of 60–100 nm, depending on the measurement technique.

On the basis of the above discussion, not only is it essential to define the required scanned area for surface roughness measurements already during the design stage, it is also advisable to define by what technique (or techniques) the roughness of medical devices should be determined. Statistical and fractal analysis approaches can help in eliminating scaling effects.[35,36] However, these approaches are not mature enough yet, and are still subject to debate. Real differences of the order as those reported in this work could affect not only the aesthetics, but also the tribological behavior, corrosion resistance and biocompatibility of implants. Therefore, there seems to be an urgent need for ISO/ASTM standard for roughness measurements of small metal parts by means of AFM.

The effectiveness of pulse EP should be discussed in light of the results reported so far. If charge is transferred in short pulses, the Nernst diffusion layer would be thinner than under DC conditions because the full thickness of the layer does not have time to develop before the pulse terminates. The shorter the pulse used, the more the current distribution is determined by primary current distribution conditions, where the Ohmic solution resistance - which is determined by the specific resistivity of the solution and by the configuration of the cathode and the anode with respect to each other as well as their respective shapes - is the largest resistance in the system. Short pulses may also allow the current distribution to be controlled by secondary current distribution (activation controlled) conditions, where the Faradaic (charge-transfer) resistance is the largest resistance in the system.[10] The use of short pulses of current can thin the effective Nernst diffusion layer so much, that a micro-profile can become a macro-profile, or a macro-profile can become a smaller macro-profile, thus reducing the concentration polarization. For regions having only micro-asperities, or when the macro-asperities become micro-asperities, the distribution of the electrolytic activity is affected by the rate of mass transport through the diffusion layer, which causes the effect of the electric current to be more uniform. Such a condition is known as tertiary current distribution. Consequently, smoothing of a surface with micro-asperities requires longer pulses (or even DC), shorter off-times, and reduced agitation. It is likely that the surface finish obtained in the current work via pulse EP could be improved by applying a finer pulse profile, say, current on-time no longer than 100 μs, current off-time 10 μs to 500 ms, and a ratio between the on-time and off-time equals 0.001 to 0.1. Alternatively, periodic reverse pulsed voltage (or current) profiles could provide further improvement of surface finish. During the backward (negative) pulses, hydrogen molecules in gas bubbles adjacent to the cathode surface (that are generated during the positive, forward, pulses) can be dissociated, whereas reduction of either nascent oxygen or passive layers at the surface of the workpiece can occur. Consequently, the adverse effects of bubble formation within the inter-electrode gap can be eliminated (or, at least, minimized), and the polishing may become more uniform on the microscopic level.[27,28] Obviously, these anticipated improvements should be verified by a careful study of the system of interest, i.e. the relevant combination of workpiece material and electrolyte solution.

As mentioned in the previous section, XRD was performed on selected samples to identify possible effects of the EP processes on the microstructure of the top layers of the bar material and the level of residual micro-strains (or micro-stresses). The microstructure of all four types of samples was found to be consisted of austenite, as expected from 316LVM

stainless steel. No evidence for martensite (which could be formed during severe plastic deformation) or ferrite (which could remain as a residue from the high-temperature production processes of the material) was found. All four types of bars were found to have a [220] preferred orientation. The lattice parameters were similar in all four types of samples, with no significant difference. No meaningful indications for changes in the levels of micro-strains and micro-stresses were observed. Because the difference in the FWHM values became more significant at low-angle reflections (the values for the (111) reflection being smaller for the DC-EP and pulse EP samples, larger for the US-EP sample, and much larger for the unpolished sample), it was concluded that the width of the peak was controlled mainly by grain size, and less by micro-strains. Specifically, the grain size was estimated to be finer in the top layers of the DC-EP and pulse-EP materials, compared to the US-EP and unpolished materials. However, additional high-resolution XRD studies are required to determine the effect of different EP processes on micro-strains and micro-stresses in a more sensitive manner.

The animal studies performed did not show considerable differences between the body reaction to the four analyzed types of bars. In all sections there was evidence of suture material surrounded by macrophages, multinucleated giant cells, and fewer lymphocytes. Adjacent to this area there was a void space (interpreted as the implant site), surrounded by a fragmented capsular structure (fragmentation was artifactual because of removal of implant), that varied in thickness and cellular component in all sections. The maximum thicknesses of the capsule ventral (i.e. towards the muscle) and capsule dorsal (i.e. towards the skin) were measured in the US-EP bar, and found to be 25 and 70 μm, respectively. These are considered small capsule thicknesses, and indicate moderate body reaction. The capsule surrounding the rod was apparently the thickest at the site of the suture material. Within the second section, away from the suture material, the capsule was unidentifiable in some cases. In all samples, there was a linear area of fibrosis parallel and between the adipose panniculus and the skeletal muscle. This band of fibrous tissue was infiltrated by few mononuclear cells and rare multinucleated giant cells surrounding free fragments of hair. The inflammatory reaction observed appeared to be incited by the suture material holding the implant in place and the method of implantation (dissection of subcutaneous tissue), rather than the implant itself. Thus, based on these initial animal studies it was concluded that all four types of bars have the potential of performing well *in vivo*, at least on the short term (as indicated by the similar, small capsule thicknesses). Yet, these animal studies should be extended to extract more reliable, statistically significant, data.

To better estimate the versatility of the pulse EP process and its applied potential in the market of biomedical devices, it was practiced also on the Ex-PRESS™ Mini Glaucoma Shunt from Optonol (Neve Ilan, Israel). Glaucoma is a chronic disease usually characterized by an increase in the intraocular pressure (IOP). This might, in time, result in damage to the optic nerve, loss of peripheral or side vision, and ultimately blindness. The higher the pressure within the eye, the greater the chance of damage to the optic nerve. The device is implanted under a scleral flap and provides a simplified method of filtration surgery for patients with open-angle glaucoma. Similar to trabeculectomy, the shunt reduces the IOP by diverting the aqueous humor from the anterior chamber to the subconjunctival space to form a filtration bleb. Post-op aqueous outflow is controlled by the flow-modulating design and the scleral flap.

The device is made of 316LVM stainless steel. A penetrating tip enables optimal insertion with minimal damage to tissues. The main shaft is 0.4 mm in outer diameter and 3-mm long. An axial orifice serves as the main fluid conduit. A spur prevents extrusion, while an external plate prevents intrusion and occlusion. The manufacturing processes include electrical discharge machining (EDM) for cutting and hole-drilling. Joining of parts is made by laser welding. Both processes might introduce metallurgical inhomogeneities. Figure 7(a) provides a macroscopic view of the rough surface and welding signs at the stage of manufacturing. To achieve good performance of the device, a fine surface finish is required. However, EP of this device is challenging because of the complex shape, small dimensions and metallurgical nonuniformities. The standard DC-EP process

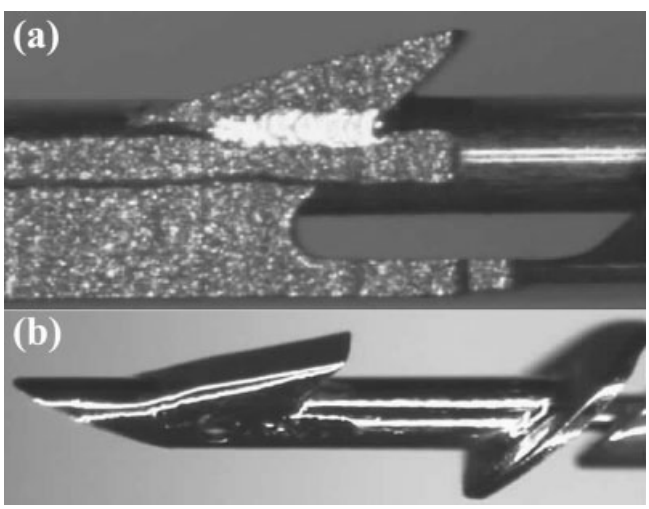

Figure 7. Macroscopic view of the Ex-press™ Mini Glaucoma Shunt device (a) before, and (b) after pulse EP.

had been tried and found to result in accelerated material removal at the welding zones, over-sizing of holes, unwanted rounding of the sharp edges, and unsatisfactory polishing of the EDM rough zone. Pulse EP, on the other hand, was found to provide very good surface finish (even without prior mechanical polishing), which was approved by strict quality assurance protocols. Figure 7(b) shows one of the pulse-EP devices. The surface of the pulse-EP device is brighter than that of a mechanically polished device. The polishing looks macroscopically uniform, sharp edges are maintained, the holes are not excessively enlarged, and the welding zone is not exposed. Hence, it is concluded that pulse-EP seems to be an attractive alternative to the current manufacturing process. Further work, such as corrosion tests and *in vivo* studies, is still to be carried out in this direction.

CONCLUSIONS

In the market of biomedical devices, there is interest in either smoothing or roughening and texturing of surfaces, depending on the desired level of body response. Electropolishing of modern miniature surgical implants involves new challenges, and stimulates the development of innovative processes. In this study, two innovative electropolishing techniques (namely, pulse electropolishing and ultrasonic electropolishing) were studied on two types of implants made of 316LVM stainless steel, and compared to the standard DC-electropolishing process. The following conclusions were drawn:

1. Pulse electropolishing is effective in eliminating the marks of gas bubbles on the workpiece and extending the working conditions range. Although the surface roughness was similar to that achieved by standard DC-electropolishing, optimization of the pulse profile is likely to result in improved surface finish.
2. Ultrasonic electropolishing yielded a fairly uniform, patterned (cratered) surface, which may be attractive for applications of osseointegration or surface preparation for electrodeposition.
3. X-day diffraction did not reveal significant differences between samples with respect to micro-strains and micro-stresses. Possibly, high-resolution diffraction tests, with higher sensitivity, are required to detect such differences.
4. A significant difference was found between the amplitude surface roughness values obtained by AFM and by noncontact surface profilometer. Not only do these differences result from different scanning areas, they are also affected the physical principals of each technique. The differences observed were large enough to affect the pass/fail decision in quality control. Therefore, not only is it essential to define the required scanned area for surface roughness measurements already during the design stage, it is also advisable to define by what technique/s the roughness of medical devices should be determined. There seems to be an urgent need for a test-method standard for roughness measurements of small metal parts by means of AFM.

References

1. Shchigolev PV. Electrolytic and Chemical Polishing of Metals. Holon: Freund; 1970.
2. Metals Handbook, Vol. 5: Surface Cleaning, Finishing, and Coating, 9th ed. Ohio: ASM; 1982. p303.
3. Metals Handbook, Vol. 9: Metallography and Microstructures, 9th ed. Ohio: ASM; 1982. p48.
4. ASTM F 86-01: Standard practice for surface preparation and marking of metallic surgical implants. Pennsylvania: ASTM; 2001.
5. ASTM B 912-02: Standard specification for passivation of stainless steel using electropolishing. Pennsylvania: ASTM; 2002.
6. ASTM A 967-01: Standard specification for chemical passivation treatment for stainless steel parts. Pennsylvania: ASTM; 2001.
7. http://www.pipingnews.com/fda%20Definitions.htm.
8. ASTM E 1558-99: Standard guide for electrolytic polishing of metallographic specimens. Pennsylvania: ASTM; 1999.
9. Bockris JO'M, Reddy AKN. Modern Electrochemistry, Vol. 1. New York: Plenum; 1970. p 379, 550.
10. Eliaz N, Gileadi E.Induced codeposition of alloys of tungsten, molybdenum and rhenium with transition metals. In: Vayenas CG, White RE, editors. Modern Aspects of Electrochemistry, Vol. 42. Berlin: Springer; 2007.
11. Jacquet PA. On the anodic behavior of copper in aqueous solutions of orthophosphoric acid. Trans Electrochem Soc 1936; 69:629–655.
12. Elmore WC. Electrolytic polishing. J Appl Phys 1939;10:724–727.
13. Elmore WC. Electrolytic polishing. II. J Appl Phys 1940; 11:797–799.
14. Baumann F, Ginsberg H. Aluminium (BRD) 1956;32:706.
15. Edwards J. The mechanism of electropolishing of copper in phosphoric acid solutions. J Electrochem Soc 1953;100:189C–194C.
16. Wagner C. Contribution to the theory of electropolishing. J Electrochem Soc 1954;101:225–228.
17. Jacquet PA. Electrolytic polishing of metallic surfaces. Metal Finish 1949;47:48–54.
18. Ratner BD, Hoffman AS, Schoen FJ, Lemons JE, editors. Biomaterials Science—An Introduction to Materials in Medicine, 2nd ed. California: Academic Press; 2004. p 3.
19. Eliaz N. Biomaterials and corrosion. In: Mudali UK, Raj B, editors. Corrosion Science and Technology. Ohio: ASM; 2007.
20. ASTM F 138-03: Standard specification for wrought 18Cr-14Ni-2.5Mo stainless steel bar and wire for surgical implants (UNS S31673). Pennsylvania: ASTM; 2003.
21. Percutaneous valve technologies: European cardiologists offer new horizons in percutaneous valve replacements. HeartWire, May 31, 2002.

22. de Scheerder I, Sohier J, Verbeken E, Froyen L, van Humbeeck J. Biocompatibility of coronary stent materials: Effect of electrochemical polishing. Mat-wiss u Werstofftech 2001;32: 142–148.
23. Zhao H, van Humbeeck J, Sohier J, de Scheerder I. Electrochemical polishing of 316L stainless steel slotted tube coronary stents. J Mater Sci Mater Med 2002;13:911–916.
24. Engineering surfaces to enhance cell adhesion. Mater Today 2003;6:19.
25. Hocheng H. US Patent 6,315,885, November 13, 2001.
26. Burstein GT, Hutchings IM, Sasaki K. Electrochemically induced annealing of stainless-steel surfaces. Nature 2000; 407:885–887.
27. Taylor EJ. US Patent 6,558,231, May 6, 2003.
28. Zhou C, Taylor EJ, Sun JJ, Gebhart LE, Renz RP. US Patent 6,402,931 B1, June 11, 2002.
29. Abbott EJ, Firestone FA. Specifying surface quality. Mech Eng 1933;55:569–572.
30. ASTM F 1438-93(99): Standard test method for determination of surface roughness by scanning tunneling microscopy for gas distribution system components. Pennsylvania: ASTM; 1993.
31. ISO 13565-2:1996: Geometrical product specifications (GPS)—Surface texture: Profile method; Surfaces having stratified functional properties, Part 2: Height characterization using the linear material ratio curve. Geneva: ISO; 1996.
32. Rohly K, Istephanous N, Belu A, Untereker D, Coscio M, Heffelfinger J, Thomas R, Allen J, Francis R, Robinson A, Perron N, Sahli B, Kobielush B. Effect of time, temperature and solution composition on the passivation of 316L stainless steel for biomedical applications. Mater Sci Forum 2003;426/432:3017–3022.
33. Kühle A, Rosén BG, Garnaes J.Comparison of roughness measurement with atomic force microscopy and interference microscopy. In: Duparre A, Singh B, editors. Proc SPIE, Vol. 5188. Washington: SPIE; 2003. p 154.
34. Bourauel C, Fries T, Drescher D, Plietsch R. Surface roughness of orthodontic wires via atomic force microscopy, laser specular reflectance and profilometry. Eur J Orthod 1998;20:79–92.
35. Martan J, Przybylski G, Tabaka R, Kowalski ZW. Fractal analysis of roughness profile induced by ion bombardment of metal surface. Vacuum 2005;78:217–221.
36. Kogut L, Jackson RL. A Comparison of contact modeling utilizing statistical and fractal approaches. J Tribol 2006;128:213–217.